Hofstadter butterfly in transistion metal dichalcogenide monolayers

Presenter
Tran Khoi Nguyen [1]

Supervisors
Dr. Huynh Thanh Duc [2]

[1]University of Science, Ho Chi Minh city

[2]Institute of Applied Mechanics and Informatics

Jul, 2025

Table of Contents

Overview

Group VI-B Transition Metal Dichalcogenides (TMD) are compound semiconductors of the type MX_2

MX_2
M: Transition metal
X: Chalcogenide

Figure: Transition metal dichalcogenides compound.

Transition Metal Dichalcogenides Monolayers

- One M layer sandwiched by two X layers as show in top view (a) and side view (b).

- Crystal structure has no central inversion symmetry.

- The symmetry of the lattice results in the hexagon Brillouin Zone (BZ).
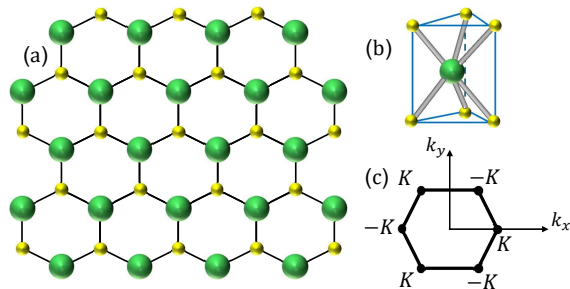

Figure: Structure and Brillouin Zone of Monolayer TMD, redrawing from[1].

---

[1] Liu et al., "Three-band tight-binding model for monolayers of group-VIB transition metal dichalcogenides".

Transition Metal Dichalcogenides Monolayers

Properties

- Both mono-layer and few-layers remain stable at room temperature.
- TMD monolayer has the visible band gap in the ban structure, which can be used in creating the transistor devices[2].
- Strong spin-orbit coupling (SOC) in TMD monolayers lead to spin splitting of hundres meV.

$\Rightarrow$ Promising material in electronic and optoelectronic applications.

---

[2] Radisavljevic et al., "Single-layer MoS2 transistors"

Three-band tigh-binding model without magnetic field

Time-independent Schrödinger equation for an electron in the crystal

$$\left[-\frac{\hbar^2 \boldsymbol{\nabla}^2}{2m} + U_0(\mathbf{r})\right] |\psi_{\lambda,\mathbf{k}}(\mathbf{r})\rangle = \epsilon_{\lambda,\mathbf{k}} |\psi_{\lambda,\mathbf{k}}(\mathbf{r})\rangle. \tag{1}$$

Tight-binding (TB) wave function

$$|\psi_{\lambda,\mathbf{k}}(\mathbf{r})\rangle = \sum_j C_j^{\lambda}(\mathbf{k}) \sum_{\mathbf{R}} e^{i\mathbf{k}\cdot\mathbf{R}} |\phi_j(\mathbf{r}-\mathbf{R})\rangle. \tag{2}$$

The basis consists of three d-orbitals of the M atom:

$$|\phi_1\rangle = |d_{z^2}\rangle, |\phi_2\rangle = |d_{xy}\rangle, |\phi_3\rangle = |d_{x^2-y^2}\rangle. \tag{3}$$

The coefficents $C_j^{\lambda}(\mathbf{k})$ are the solutions of the eigenvalue equation

$$\sum_{jj'}^{3} \left[H_{jj'}^{\mathsf{TB}}(\mathbf{k}) - \varepsilon_{\lambda}(\mathbf{k})S_{jj'}(\mathbf{k})\right] C_j^{\lambda}(\mathbf{k}) = 0. \tag{4}$$

Three-band tigh-binding model without magnetic field

Overlap matrix elements

$$S_{jj'}(\mathbf{k}) = \sum_{\mathbf{R}} \left\langle \phi_j(\mathbf{r}) \middle| \phi_{j'}(\mathbf{r} - \mathbf{R}) \right\rangle \approx \delta_{jj'}. \tag{5}$$

TB Hamiltonian matrix elements

$$H_{jj'}^{\mathsf{TB}}(\mathbf{k}) = \sum_{\mathbf{R}} e^{i\mathbf{k}\cdot\mathbf{R}} \left\langle \phi_j(\mathbf{r}) \middle| \left[-\frac{\hbar^2 \nabla^2}{2m} + U_0(\mathbf{r}) \right] \middle| \phi_{j'}(\mathbf{r} - \mathbf{R}) \right\rangle. \tag{6}$$

Three-band tigh-binding model without magnetic field
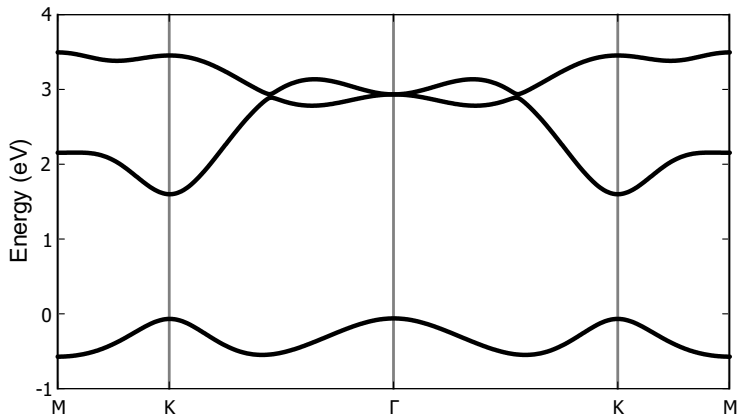
Figure: Band structure of MoS_2 monolayer[3].

[3] Liu et al., "Three-band tight-binding model for monolayers of group-VIB transition metal dichalcogenides".

Three-band tigh-binding model under a magnetic field

TB Hamiltonian matrix elements change to

$$H = \frac{(-i\hbar\boldsymbol{\nabla} + e\mathbf{A}(\mathbf{r}))^2}{2m} + U_0(\mathbf{r}) + g^*\mu_B\mathbf{B}\cdot\mathbf{L}, \tag{7}$$

It is possible to add a phase factor to the basis functions

$$\psi_{\lambda,\mathbf{k}}(\mathbf{r}) = \sum_{j=1}^{3} C_j^\lambda(\mathbf{k}) \sum_{\mathbf{R}} e^{i(\mathbf{k}\cdot\mathbf{R}+\theta_{\mathbf{R}}(\mathbf{r}))}\phi_j(\mathbf{r}-\mathbf{R}). \tag{8}$$

By choosing $\theta_{\mathbf{R}} = -\frac{e}{\hbar}\int_{\mathbf{R}}^{\mathbf{r}}\mathbf{A}(\mathbf{r}')\cdot d\mathbf{r}'$ as Peierls substitution, the Hamiltonian matrix elements as the form

$$\begin{aligned}
H_{jj'}^{\mathsf{TB}}(\mathbf{k}) = &\sum_{\mathbf{R}} e^{i\mathbf{k}\cdot\mathbf{R}+\frac{ie}{\hbar}\int_{\mathbf{0}}^{\mathbf{R}}\mathbf{A}(\mathbf{r}')\cdot d\mathbf{r}'} \langle\phi_j(\mathbf{r})|\left[-\frac{\hbar^2\boldsymbol{\nabla}^2}{2m} + U_0(\mathbf{r})\right]|\phi_{j'}(\mathbf{r}-\mathbf{R})\rangle \\
&+ g^*\mu_B\mathbf{B}\cdot\sum_{\mathbf{R}} e^{i\mathbf{k}\cdot\mathbf{R}+\frac{ie}{\hbar}\int_{\mathbf{0}}^{\mathbf{R}}\mathbf{A}(\mathbf{r}')\cdot d\mathbf{r}'} \langle\phi_j(\mathbf{r})|\mathbf{L}|\phi_{j'}(\mathbf{r}-\mathbf{R})\rangle.
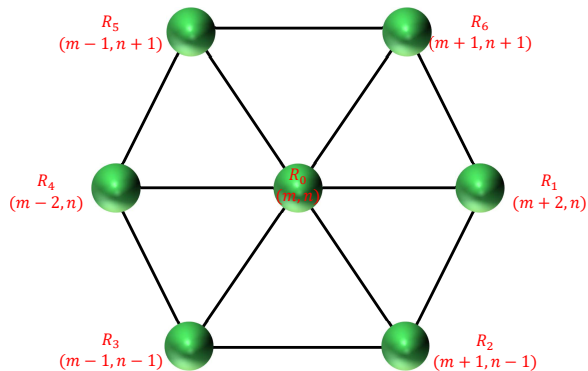\end{aligned} \tag{9}$$

Figure: The TB model of TMDC with six neighbors atom M.

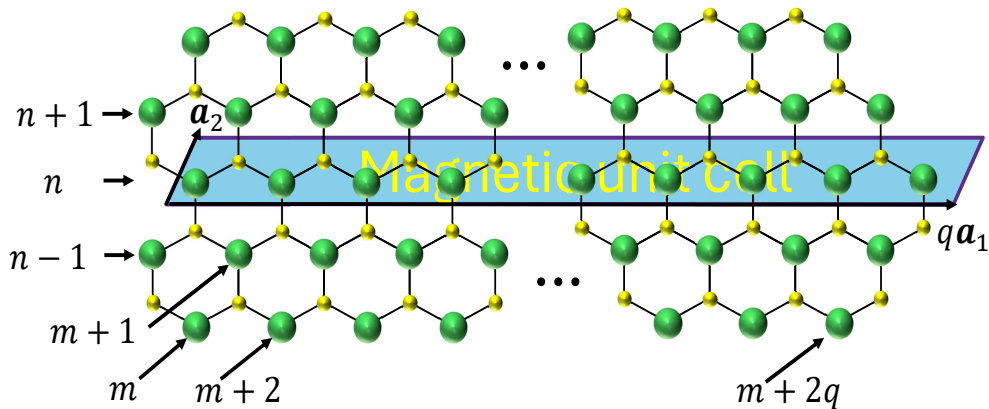# Three-band tigh-binding model under a magnetic field

Figure: Magnetic unit cell for TMD monolayers.

Three-band tigh-binding model under a magnetic field

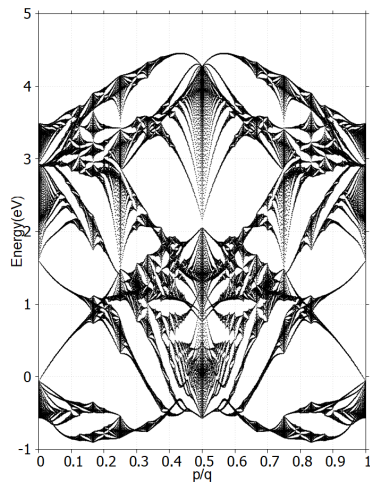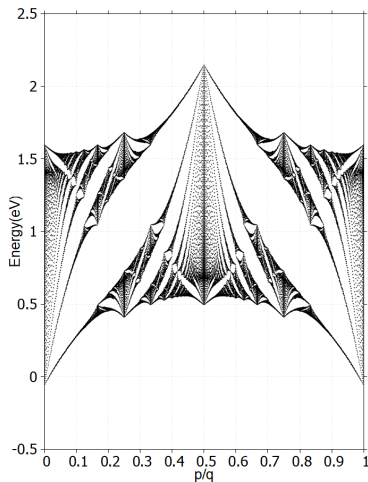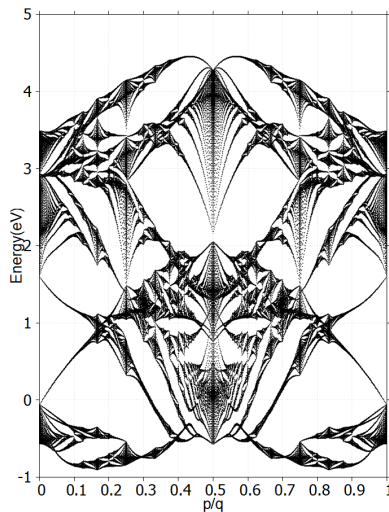Figure: Hofstadter butterfly for single-band $|dz\rangle \equiv |\phi_1^1(x,y)\rangle$(left) and three-band(right) with $q = 797$ with field strength $B_0 = 4.6928 \times 10^4$ T.
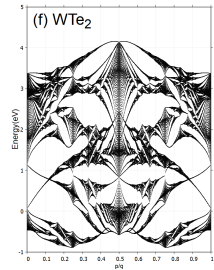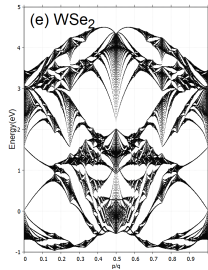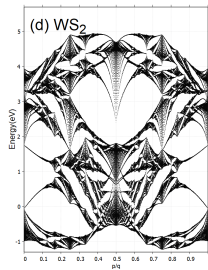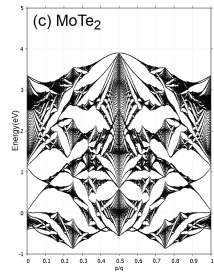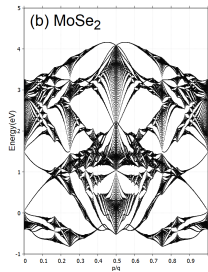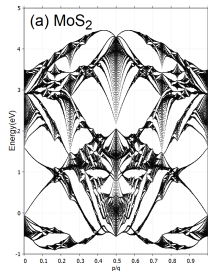
Hofstadter butterfly

Properties

-
-
- The spectrum also invariant under reversal of the magnetic field $\frac{p}{q} \to -\frac{p}{q}$.
- At weak magnetic field, Landau levels can clearly seen from the Hofstadter spectrum.

Hofstadter butterfly in MX_2

(a) MoS$_2$ (b) MoSe$_2$ (c) MoTe$_2$ (d) WS$_2$ (e) WSe$_2$ (f) WTe$_2$
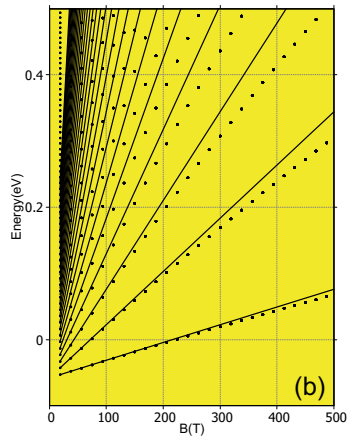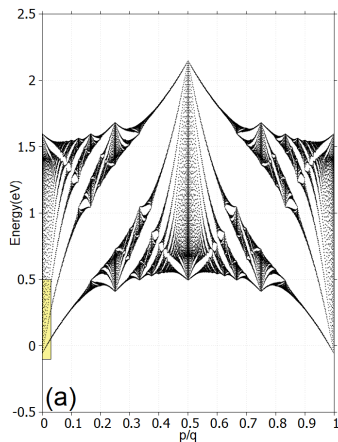
Landau levels

Figure: (a) Same plot as Fig (2.6) but considering a small area and (b) shows superposition of the Landau fan diagram and the Hofstadter butterfly. Display the first $n = 30$ levels near the bottom of the conduction band for a magnetic field up to $B = 500$ T.

Classical Hall effect

Summary:

- We confirm the Hofstadter butterfly in this model corrected compared to previous study.
- From three-band TB + magnetic field $\rightarrow$ QHE.

Further research:

- High Harmonic Generation
- High-order Side-band Generation
- Photovoltaic effect

Thank you for your listening.